



Scripta Materialia 65 (2011) 695-698



www.elsevier.com/locate/scriptamat

Tension behavior of free-standing amorphous film and amorphous crystalline nanolaminates in submicron scale

C.J. Lee, a,* H.K. Lin, b,c J.C. Huang and S.Y. Kuan

^aDepartment of Materials and Optoelectronic Science, Center for Nanoscience and Nanotechnology, National Sun Yat-Sen University, Kaohsiung 804, Taiwan

^bLaser Application Technology Center/Industrial Technology Research Institute South (ITRI South), Liujua Shiang 734, Taiwan

^cChina Steel Corporation, Kaohsiung 812, Taiwan

Received 23 February 2011; revised 5 July 2011; accepted 7 July 2011 Available online 14 July 2011

Free-standing amorphous ZrCu film and amorphous—crystalline ZrCu/Cu nanolaminates are subjected to membrane deflection experiments to investigate their tensile deformation. The ZrCu specimen exhibits poor deformability with brittle fracture. In comparison, moderate plasticity occurs for the nanolaminates, and the plasticity increases as the thickness of the individual layers decreases from 100 down to 25 nm. The ZrCu/Cu nanolaminates with a layer thickness of 25 nm exhibit a fracture angle close to 45° and a dimpled fracture surface, implying moderate tensile ductile fracture.

© 2011 Acta Materialia Inc. Published by Elsevier Ltd. All rights reserved.

Keywords: Tensile deformation; Amorphous thin film; Free-standing film; Nanolaminate; Multilayer

Improving the ductility of metallic glasses (MGs) has always been a critical issue. Proposed approaches for improving plasticity include the concept of intrinsic [1-5]or extrinsic [6-8] metallic glass composites (MGCs), as well as nano- and microscaled phase separation [9,10]. For monolithic MGs or MGCs, compressive plasticity has been demonstrated by a large number of studies. There have been fewer studies, however, on tensile ductility, where the initial cracking of shear bands is confined throughout the entire tensile specimens, so that they exhibit plasticity beyond the elastic limit. It has been suggested that some soft crystalline precipitates introduced into the MG matrix are responsible for this, and that the spacing (or length scale) between such crystalline obstacles is an important parameter for the plastic shielding of an opening crack tip to limit the extension of the shear band.

Nanolaminate structures of crystalline materials can be used to study the characteristics of nanocrystalline materials [11], and these amorphous—crystalline multilayers or nanolaminates are also feasible routes by which to improve the MG plasticity, especially under tensile deformation. Nieh et al. [12] and Wang et al. [13] synthesized amorphous CuZr (5 nm thick)/crystalline Cu

(35 nm thick) nanolaminates via sputter processing. The nanolaminates exhibited outstanding tensile ductility (10-15% strain) at room temperature and a high strength of ~1.1 GPa. Also, the amorphous PdSi (10 nm thick)/crystalline Cu (90 nm thick) nanolaminates fabricated by Donohue et al. [14] could be rolled to a 60-80% thickness reduction without fracture or formation of major fatal shear bands. These aforementioned amorphous-crystalline nanolaminates possessing thin amorphous layers (typically thinner than the \sim 25 nm width of the shear band) and sufficiently thick and stiff crystalline layers can suppress the formation of principal shear bands, giving them superior ductility. However, in the previously reported cases, the crystalline layers occupy an overall volume fraction greater than 80%. These nanolaminates should thus be termed as crystalline-base composites, rather than metallic glass composites. It is of interest to see if nanolaminates with an amorphous phase volume fraction of 50% or above can still show good tensile ductility. It is important to ascertain whether such outstanding plasticity can be retained under tensile deformation.

For most reported studies on film tension [15–17], the facile measurement of tensile deformation for the thin film materials was conducted directly by coated uniaxial tensile specimens with a polymer or silicon substrate. Another method is to perform a bending test and

^{*}Corresponding author. Tel.: +886 7 5254070; fax: +886 7 5254099; e-mail: leechingjen@gmail.com

examine the tension-side deformation [18]. Nevertheless, the interface properties between the substrate and the film would influence the mechanical behavior of the coated films during deformation [15,16,19,20]. In the literature, a number of tensile testing designs have been developed for free-standing films, including the bulge test [21,22], microbeam bending [21,22] and the membrane deflection test [23]. In this study, the membrane deflection method is employed to study free-standing and amorphous—crystalline nanolaminates with various layer thicknesses.

(100) Si wafers that had undergone double-sided polishing were first covered on both sides with a layer of ~550 nm Si₃N₄ film, deposited by low-pressure chemical vapor deposition, to act as a protective membrane during the subsequent wet etching of the wafers. Some portions of the Si₃N₄ layer were removed with a pulsed ultraviolet laser on the bottom side of Si wafer to form a pattern of etching windows. The pre-processed Si wafers were cleaned in an ultrasonic cleaner for 5 min with deionized water, ethanol and acetone, then dried with nitrogen gas. After the cleaning process, the ZrCu amorphous layers and Cu nanocrystalline layers were deposited sequentially onto the top side of each pre-processed Si wafer. The volume fraction of ZrCu and Cu was fixed to 50%. Samples with ZrCu/Cu thickness of 100/100, 50/50 and 25/25 nm, and a monolithic ZrCu layer - referred to as ZCC-100, ZCC-50, ZCC-25, and ZC, respectively - were fabricated, and the overall thickness of the ZrCu/Cu nanolaminates was kept at about 1 μm. Wet etching in 40% KOH solution and dry etching in CF₄ and O₂ plasma were utilized to remove the Si substrate and Si₃N₄ layer below the ZrCu/Cu nanolaminates, respectively.

The free-standing nanolaminates were subsequently machined to form a dogbone-shaped bridge specimen with a focused ion beam (FIB). The half length of the bridge span, the gage length of the dogbone-shaped specimen and the width of bridge were about 65–75, 40–50 and 7 μm, respectively. A Berkovich tip was indented onto the central part of the dogbone-shaped bridge specimen to induce tensile deformation in an MTS XP nanoindenter. The method used followed the membrane deflection experiment [24]. The loading rate control mode of the basic mode was adopted during the indentation. The loading rate and maximum load were 5×10^{-3} mN s⁻¹ and 5 mN, respectively. The fracture morphology was characterized by scanning electron microscopy (SEM), and the laminated structures of the as-deposited and deformed samples we examined by transmission electron microscopy (TEM).

Figure 1 shows the typically dogbone-shaped bridge specimens for ZCC-100 and ZCC-25 before and after indentation. Due to the residual stress of the as-deposited films, the free-standing membrane dogbone-shaped specimens are typically bent very slightly in the as-FIB-machined condition.

The dogbone-shaped specimens were all loaded by the indenter, and the free-standing membrane underwent tensile deformation until failure. Figure 2 shows the raw curves of load (*p*)—displacement (*h*) data. The curves of ZC, ZCC-100 and ZCC-50 all have an inverted L shape, with a lower slope in stage I and a higher slope

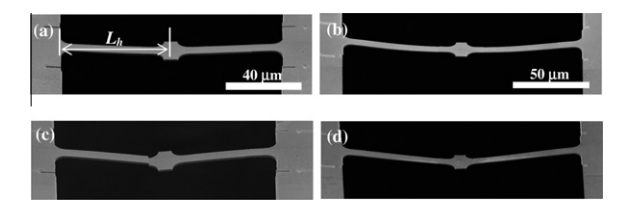


Figure 1. SEM micrographs showing the dogbone-shaped bridge specimens of ZCC-100 and ZCC-25: (a and b) before indentation and (c and d) after indentation, respectively.

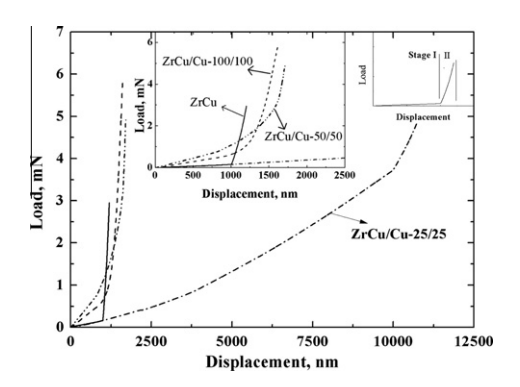


Figure 2. Raw load–displacement curves of the membrane deflection experiment for the ZC, ZCC-100, ZCC-50 and ZCC-25 specimens.

Table 1. Comparison of the slopes, deformability index and fracture stress of the four different free-standing specimens.

	ZC	ZC-100	ZC-50	ZC-25
Stage I slope (mN nm ⁻¹)	1.5×10^{-4}	6.1×10^{-4}	9.3×10^{-4}	-
Stage II slope (mN nm ⁻¹)	0.015	0.016	0.020	-
Deformability index (%)	1.4	2.2	2.4	>15
Fracture stress (GPa)	0.6	2.0	2.5	2.5

in stage II, as shown clearly in the inset of Figure 2. In contrast, ZCC-25 does not show this shape, exhibiting a near-power-law curve. In order to simplify the description of the inverted L shape, these curves for stages I and II were fitted by linear lines, and their extracted slopes are listed in Table 1.

These inverted L curves imply that the bridges were subjected to a tensile force on two sides of the indenter for stage I. With increasing indentation force, one side of the bridge would eventually break, resulting in a change of deformation mode from tensile deformation on two sides (stage I) to bending deformation of the one remaining side without breaking (stage II). Due to this change in deformation mode, the specimen stiffness would exhibit the sudden inflection. Note that the stage II slopes of the ZC, ZCC-100 and ZCC-50 specimens in Figure 2 are all nearly identical. Moreover, another phenomenon noted is that the slope of stage I gradually increased from ZC to ZCC-100 to ZCC-50, implying that the hardening rate during tensile deformation increased with decreasing layer thickness for layer thicknesses greater than 50 nm.

Download English Version:

https://daneshyari.com/en/article/1499692

Download Persian Version:

https://daneshyari.com/article/1499692

<u>Daneshyari.com</u>